LBL-16736 c.2

Lawrence Berkeley Laboratory
UNIVERSITY OF CALIFORNIA

Physics, Computer Science & Mathematics Division

To be published in the Proceedings of the 11th Stanford Linear Accelerator Center Summer Institute on Particle Physics, Stanford, CA, July 18-29, 1983

SEARCH FOR RIGHT-HANDED CURRENTS IN MUON DECAY

D.P. Stoker

September 1983

RECEIVED
NOV 1 1983
L.B.L. LIBRARY

Prepared for the U.S. Department of Energy under Contract DE-AC03-76SF00098

LBL-16736 c.2

DISCLAIMER

This document was prepared as an account of work sponsored by the United States Government. While this document is believed to contain correct information, neither the United States Government nor any agency thereof, nor the Regents of the University of California, nor any of their employees, makes any warranty, express or implied, or assumes any legal responsibility for the accuracy, completeness, or usefulness of any information, apparatus, product, or process disclosed, or represents that its use would not infringe privately owned rights. Reference herein to any specific commercial product, process, or service by its trade name, trademark, manufacturer, or otherwise, does not necessarily constitute or imply its endorsement, recommendation, or favoring by the United States Government or any agency thereof, or the Regents of the University of California. The views and opinions of authors expressed herein do not necessarily state or reflect those of the United States Government or any agency thereof or the Regents of the University of California.

SEARCH FOR RIGHT-HANDED CURRENTS IN MUON DECAY*

D.P. Stoker

Lawrence Berkeley Laboratory and Department of Physics
University of California, Berkeley, California 94720.

ABSTRACT

Limits are reported on right-handed currents, based on precise measurement of the e^+ spectrum end point in μ^+ decay. Highly polarised muons from the TRIUMF "surface" beam were stopped in metal foils within a 1.1 T spin-holding longitudinal field or a 70 G spin-precessing field. For the spin-held data, the V-A rate vanishes in the beam direction at the end point. Measurement of this rate sets the 90% confidence limits $\xi P_\mu \delta/\rho > 0.9959$ and $M(W_R) > 380$ GeV, where W_R is the possible right-handed gauge boson. The μSR signal amplitude of the spin-precessed data independently sets the limits $\xi P_\mu \delta/\rho > 0.9918$ and $M(W_R) > 320$ GeV. Limits on non-(V-A) currents, familons, and composite leptons are also presented.

---

* Berkeley-LBL / Northwestern† / TRIUMF# collaboration:
J. Carr, G.Gidal, B. Gobbi†, A. Jodidio, C.J. Oram#, K.A. Shinsky,[a] H.M. Steiner, D.P. Stoker, M. Strovink, and R.D. Tripp.

a Deceased

INTRODUCTION

The Glashow-Weinberg-Salam electroweak model, based on the gauge group $SU(2)_L \times U(1)$, is at present consistent with the available experimental data. The main surviving alternative to the standard model is the left-right symmetric model with gauge group $SU(2)_L \times SU(2)_R \times U(1)$.[1]

The appeal of the left-right symmetric model is partly aesthetic. In the standard model the left-handedness of the interaction is a consequence of the choice of gauge group: left-handed fermions are assigned to doublets under $SU(2)_L$ and interact with the left-handed gauge bosons $W_L^{\pm}$. Extension of the gauge group to $SU(2)_L \times SU(2)_R \times U(1)$ restores left-right symmetry at the Lagrangian level with the addition of right-handed gauge bosons $W_R^{\pm}$ and the assignment of right-handed fermions to doublets under $SU(2)_R$.

The dominance of left-handed charged currents at present energies could then arise from a $W_L - W_R$ mass splitting which is tiny on the grand-unification scale. If the mass scale $M(W_R)$ where parity is spontaneously broken is increased to infinity the left-right symmetric model reduces to the standard model, and therefore can never be ruled out by experiments which support the standard model.

In these left-right symmetric theories the physical bosons W_1 and W_2, with mass-squared ratio $\alpha = M^2(W_1)/M^2(W_2)$, are linear combinations of the gauge bosons:

$$W_1 = W_L \cos\zeta - W_R \sin\zeta$$

$$W_2 = W_L \sin\zeta + W_R \cos\zeta$$

The effects of $W_L - W_R$ mixing and W_1 exchange relative to W_2 exchange become independent of momentum transfer for $q^2 << M^2(W_1)$. Analyses[2,3] which neglect the kinematic effect of finite ν_R mass obtain the strongest limits on α and ζ from muon and nucleon β decay.[4-9]

Unlike the standard model, in which there are only massless ν_L, the left-right symmetric model admits both ν_L and ν_R of finite mass. The ν_R mass may depend critically on whether neutrinos are Dirac or Majorana particles. In the Dirac case, ν_L and ν_R necessarily have the same mass since they are different helicity states of the same particle. In the Majorana case, as suggested by Gell-Mann, Ramond and Slansky,[10] the smallness of the ν_L mass may be related to the maximality of parity violation. Mohapatra and Senjanovic[11] find $m(\nu_L) \propto 1/M(W_R)$, and propose models in which $m(\nu_{\ell L}) \approx m_\ell{}^2/M(W_R)$ and $m(\nu_{\ell R}) \approx M(W_R)$. In these models W_R decouples from low energy leptonic processes, such as μ decay, and semileptonic processes except where the right-handed current is all hadronic.

The present experiment[12] is insensitive to right-handed currents if the ν_R masses are greater than 10 MeV. The effective low-energy interaction Hamiltonian for charged current processes with light neutrinos is:

$$H_{int} \approx [g^2/2M^2(W_1)][J_L J_L^\dagger + \alpha J_R J_R^\dagger + \zeta(J_L J_R^\dagger + J_R J_L^\dagger)]$$

The already existing experimental bounds on α and ζ are displayed as contours in Fig. 1. Only the μ decay asymmetry, which the present experiment also measures, gives a closed contour. Additional

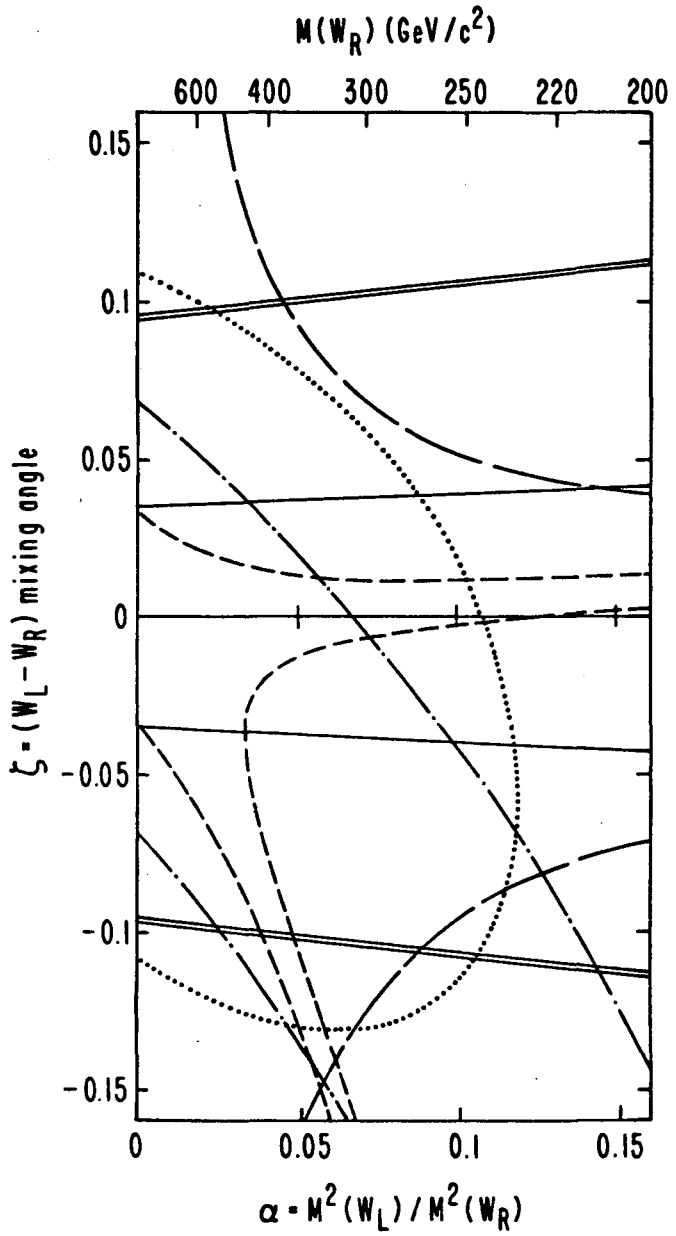

FIG. 1. Experimental 90% confidence limits on the $W_{L,R}$ mass-squared ratio α and mixing angle ζ. The allowed regions are those which include $\alpha=\zeta=0$. Muon-decay contours are derived from the polarisation parameter ξP_μ (dotted, Ref. 4), and the Michel parameter ρ (solid, Ref. 5). Nuclear β decay contours are obtained from the Gamow-Teller β polarisation (dot-dashed, Ref. 6); the comparison of Gamow-Teller and Fermi β polarisations (long-dashed, Ref. 7); and the ^{19}Ne asymmetry A(0) and ft ratio, assuming CVC (short-dashed, Ref. 8). Limits from the y distributions in νN and $\bar{\nu}N$ scattering (double-lines, Ref. 9) are valid irrespective of the ν_R mass.

constraints are placed by model-dependent calculations of the $K_L - K_S$ mass difference. Beall et al[13] found $M(W_R) > 1600$ GeV, while the later more complete calculations by DeForcrand,[14] Mohapatra et al.,[15] and Denis[16] give lower limits in the range 200 - 400 GeV.

In this experiment we observe the decay of polarised μ^+ stopped in essentially non-depolarising pure metal foils. The decays of interest are those which emit e^+ near the momentum spectrum end point $x = p_e/p_e(\max) = 1$. Neglecting radiative corrections and assuming massless neutrinos the μ^+ differential decay rate is:

$$d^2\Gamma/x^2dxd\cos\theta \propto (3-2x) + (4\rho/3-1)(4x-3) + 12(m_e x/m_\mu)(1-x)\eta - [(2x-1) + (4\delta/3-1)(4x-3)]\xi P_\mu \cos\theta \qquad (1)$$

where $\pi-\theta$ is the angle between $\hat{p}_e$ and the direction of the μ^+ polarisation P_μ, and ρ,η,δ, and ξ are the muon decay parameters.[17] The (V-A) values of the decay parameters are shown in Table 1 together with the world average experimental values. For pure (V+A) the 'asymmetry parameter' $\xi=-1$, while the other decay parameters retain their (V-A) values. Thus measurement of the decay asymmetry is a sensitive test for admixtures of right-handed currents. The (V-A) forward-backward μ^+ decay asymmetry is shown in Fig. 2.

The decay rate relative to that for unpolarised muons is

$$R(x,\theta) = 1 - \frac{1-2\tilde{x}-\tilde{\delta}+4\tilde{x}\tilde{\delta}}{1+2\tilde{x}-\tilde{\rho}+4\tilde{x}\tilde{\rho}}\,\xi P_\mu \cos\theta \qquad (2)$$

where $\tilde{x}=1-x$, $\tilde{\delta}=1-4\delta/3$, $\tilde{\rho}=1-4\rho/3$. [Radiative corrections[17] and finite electron mass effects absent from (1) and (2) are included in the actual analysis.]

TABLE 1.

The (V-A) values of the muon decay parameters and their world average experimental values.

Muon Decay Parameter	(V-A) Value	World Average Value
ρ	3/4	0.7517±0.0026
η	0	-0.12 ±0.21
δ	3/4	0.7551±0.0085
ξ	1	0.972 ±0.014

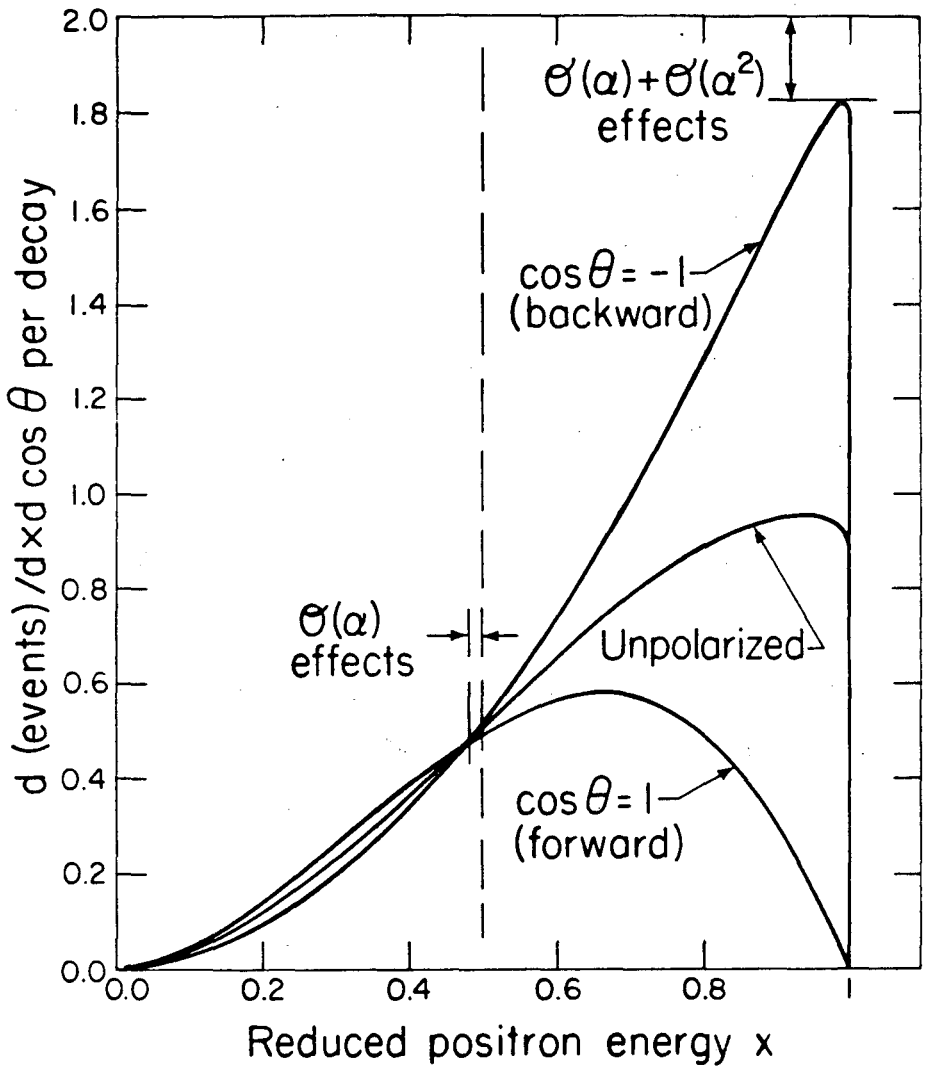

FIG. 2. The (V-A) forward-backward asymmetry in μ^+ decay. The angle between the μ^+ spin direction and the e^+ momentum is $\pi-\theta$.

The experiment was run in two modes, each of which allows determination of the decay asymmetry. In the first mode, with greater statistical power, we observe e^+ emitted near $x=1$ and also near $\theta=0$ from stopped μ^+ with their spins held in a 1.1 T longitudinal field. At the end point $R(1,0)\approx 1-\xi P_\mu \delta/\rho$ and in the (V-A) limit, $R(x\to 1,\theta\to 0)\approx 6-4x-P_\mu-\cos\theta$. For a μ^+ beam derived from π^+ decay at rest, θ becomes the angle between the e^+ and μ^+ momenta. In the (V-A) limit with massless neutrinos, angular momentum conservation requires $P_\mu=1$. In left-right symmetric theories $P_\mu\approx 1-2(\alpha+\zeta)^2$, and the end point decay rate $R(1,0)\approx 2(2\alpha^2+2\alpha\zeta+\zeta^2)$ constrains both α and ζ.

The second mode is a muon spin rotation (μSR) experiment in which the muon spins are precessed by a 70 G transverse field substituted for the 1.1 T longitudinal field. The decay asymmetry may then be determined from the amplitude of the resulting μSR signal.

EXPERIMENTAL APPARATUS

This experiment is made possible by the nearly complete polarisation of a μ^+ beam derived from π^+ decay at rest near the surface of the production target.[18] Muons from π^+ decay deeper inside the production target have lower momentum and are less polarised due to Coulomb scattering. Tuning the beam line to the surface muon edge (Fig. 3) therefore momentum selects the most highly polarised muons. The M13 beam[19] at TRIUMF produces 15,000 29.5MeV/c μ^+/sec within a 1% momentum bite and a 12×10mm spot from 100μA of 500 MeV protons incident on a 2mm thick carbon target. The 2% contamination of prompt

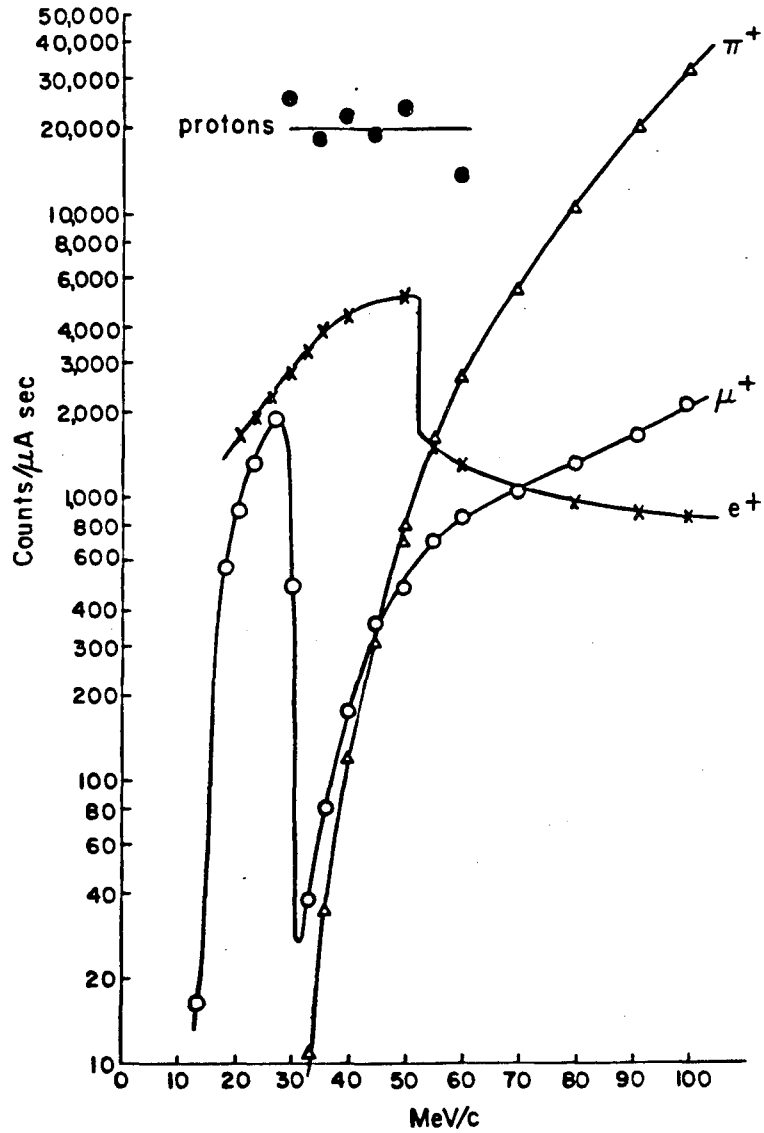

FIG. 3. Particle fluxes in the M13 beam at TRIUMF (taken from Ref. 19). The μ^+ with momenta corresponding to the sharp (surface muon) edge at 29.5 MeV/c are those produced by π^+ decay near the surface of the production target. Those with smaller momenta are from π^+ decay deeper in the production target, and are less polarised. Muons with momenta above the edge are from π^+ decay in flight near the production target.

("cloud") μ^+ from π^+ decay in flight near the production target is less polarised and is rejected by requiring the μ^+ to be produced well within the 43 nsec interval between proton bursts. A smaller π^+ flux is similarly rejected. Beam e^+, which constitute about 50% of the total flux, pass through the μ stopping target and do not satisfy the trigger requirements.

The apparatus is shown in Fig. 4. After traversing 50 mg/cm^2, beam μ^+ are stopped by target foils of ≧99.9% pure Al (155 mg/cm^2), Cu (233 mg/cm^2), Ag (275 mg/cm^2), and Au (233 mg/cm^2). The high free electron concentration in these metals screens the stopped μ^+ from prolonged spin-spin coupling to particular electrons, which otherwise would lead to its depolarisation. A 1.1 T longitudinal field (B_L) is also applied to preserve the stopped μ^+ spin direction. During alternate hourly runs the longitudinal field is nulled to within ±3 gauss and a 70 gauss transverse field (B_T) is substituted. This precesses the μ^+ spin about a vertical axis so that its time-averaged polarisation is zero.

The incoming μ^+ direction is determined using proportional chambers P1 and P2, and the outgoing e^+ direction is determined by proportional chamber P3 and drift-chambers D1 and D2. All chambers use a 92% methane - 8% methylal gas mixture. Downstream of the target the decay e^+ is focused by a 0.5 T-m solenoidal field lens. The septum between the target and solenoid bore essentially decouples the focal length from the choice of target field orientation.

The decay e^+ is momentum-analysed by an NMR-monitored cylindrical dipole magnet having a central field of 0.32 T. Low mass drift-chambers are located near its conjugate foci and the intervening

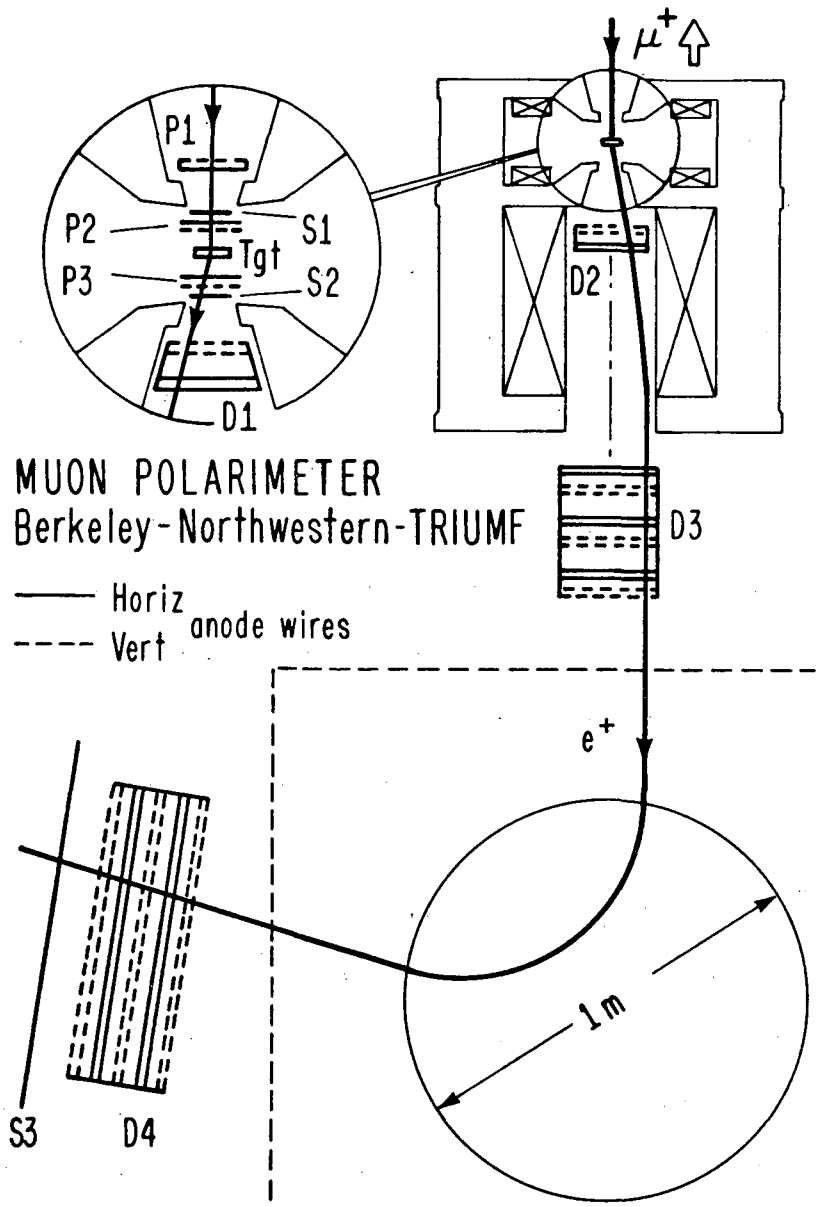

FIG. 4. Plan view of the muon polarimeter. P1-P3 are proportional wire chambers, D1-D4 are drift-chambers, and S1-S3 are scintillators. The trigger is T1•T2, where T1 is $P1 \cdot S1 \cdot P2 \cdot \overline{V1} \cdot \overline{P3} \cdot \overline{S2}$ at the μ^+ stopping time, T2 is $P3 \cdot S2 \cdot S3 \cdot \overline{P1} \cdot \overline{S1} \cdot \overline{V1} \cdot \overline{P2} \cdot \overline{V2}$ at the μ^+ decay time, and V1 and V2 are veto scintillators surrounding S1 and S2 respectively (not shown).

volume is evacuated. The dispersion $\Delta p/p\Delta s$ was measured to be 1.07%/cm by passing e^+ beams of different momenta, determined using the NMR-monitored beam line dipoles, through the spectrometer. The combined system of field lens and positron spectrometer has an acceptance of 250 msr and a momentum bite of ±20%; in the analysis described below, these are restricted to 160 msr and ±8%.

The trigger requires the signature of a beam particle stopping in the foil target, in delayed (0.2 - 10 μs) coincidence with that of a decay positron passing through the spectrometer. Events with an extra beam particle arriving between the μ-stop and decay are tagged and rejected later. The data reported here are based on 3.5×10^6 triggers from the initial run. An additional 10^7 triggers were collected later in 1982.

Incoming μ^+ tracks were reconstructed using P1 and P2. Nearly straight e^+ track segments were found separately in the horizontal and vertical projections of three groups of wire chamber planes: P3,D1,D2; D3; and D4 (Fig. 4). All possible combinations of hits were considered, and tracks in all six segments were found in 99% of the triggers. Of these, 95% had multiplicities corresponding to a single track; the remainder were rejected. Projections of the track segments were required to agree at the target, in the bore of the solenoid, and in position and vertical slope in the spectrometer. The first of these requirements rejects most of the remaining small fraction of events where the e^+ is emitted from a μ^+ other than the current μ-stop. Track segment residuals were used to dynamically fine-tune the drift-chamber space-time calibration, producing residuals of

≦250 μm in the spectrometer chambers D3 and D4.

The hits found in P1 through D2 were then fitted to curved trajectories based on the first-order optics of cylindrically symmetric fields. The μ^+ and e^+ polar angles θ_μ and θ_e with respect to the beam axis were thereby determined with resolutions of 20 and 10 mrad respectively. Monte Carlo simulation based on higher-order field optics confirms the accuracy of this procedure to within an uncertainty of ±0.0005 in $\cos\theta_\mu$ and $\cos\theta_e$. For the B_L data the transverse component of the μ^+ spin precesses about the beam axis too rapidly to be followed. Thus for $\cos\theta=-\hat{P}_\mu.\hat{p}_e$ in (2) we substitute $\cos\theta_\mu\cos\theta_e$, which is equivalent in an average over many events.

The e^+ momentum was obtained, to first order, from the measured dispersion and the sum of the horizontal coordinates at the conjugate foci of the 98° horizontally focusing spectrometer magnet. Empirical corrections to second order, based primarily on the end point position for the B_T data, were made for deviation from the median plane and impact parameter with respect to the magnet axis. The sharp edge at x=1 in Fig. 5 curve(a) exhibits a gaussian resolution which is less than 0.2% rms, with a rounded shoulder due to non-uniform energy-loss in the 180 mg/cm^2 of material upstream.

We have dropped events with $x<0.92$ or $\cos\theta<0.975$ ($\cos\theta<0.965$ for the μSR analysis), which have low statistical power for determining the decay asymmetry. After conservative fiducial cuts the final distributions in Fig. 5 retain 7.5% of the raw triggers. We have checked that any reasonable variation of the cuts would negligibly affect the the result.

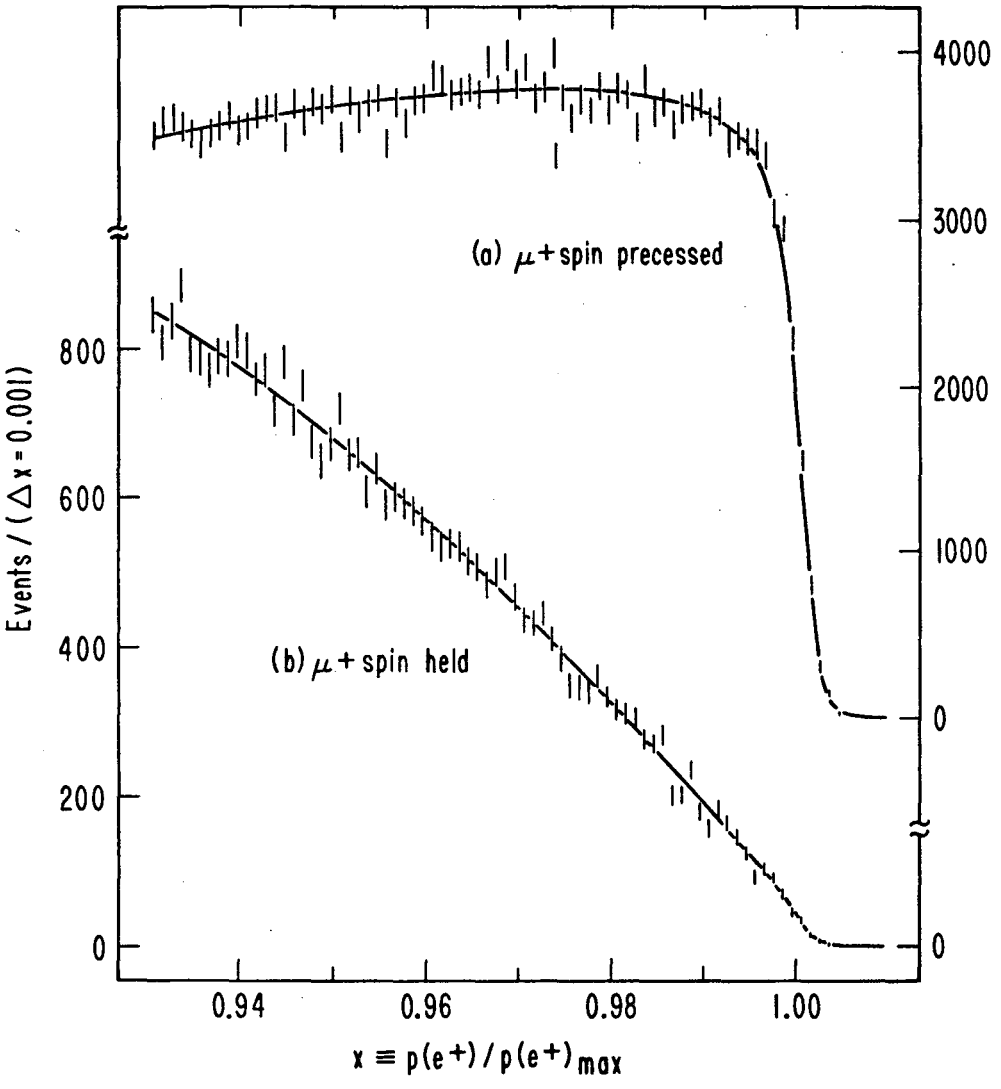

FIG. 5. Distributions (uncorrected for acceptance) in reduced positron momentum with the μ^+ spin (a) precessed and (b) held. The indicated errors are statistical. The edge in (a) corresponds to a resolution with a gaussian part <0.2% rms. The fits are described in the text.

DATA ANALYSIS

A. SPIN-HELD DATA

Fitting proceeds in two stages. The B_T data in Fig. 5(a) are fitted to the radiatively corrected spectrum expected for unpolarised μ^+ decay, smeared by a sum of gaussian resolution functions and by the expected e^+ energy-loss straggling. The fit simultaneously calibrates the edge position x=1 and determines the momentum resolution and the (quadratic) dependence of the acceptance upon x. The B_L spectrum in Fig. 5(b) can be represented as the shape expected from pure (V-A) and $P_\mu=\cos\theta=1$, with a small admixture of the unpolarised spectrum in Fig. 5(a). This unpolarised fraction is essentially equal to $1-(\xi P_\mu \delta/\rho)\langle\cos\theta\rangle$. To fit this fraction, we use the B_T fit to fix the x resolution, x acceptance, and edge position x=1, but allow the acceptance for B_L data relative to that for B_T data to vary linearly with x. This allows for the (<2%) difference in angular acceptance caused by the different field configuration near the target. Using data with partly polarised cloud μ^+, we have checked that the x=1 calibration is consistent for B_L and B_T fields. In the resulting curve in Fig. 5(b), the slight kink near x=1 reflects the unpolarised fraction, which arises mostly from the measured value $\langle\cos\theta\rangle=0.9862$ for these data.

The result reported here is based on this same fitting procedure carried out for data in each of five bins in $\cos\theta$. The subdivision checks that the results of these fits are consistent with a linear

dependence on $\langle\cos\theta\rangle$. The value of $\xi P_\mu \delta/\rho$ is determined by making a fixed slope extrapolation to $\cos\theta=1$ (see Fig. 6). Separate fits for each of the four stopping target materials (see Fig. 7) give values of $\xi P_\mu \delta/\rho$ which are statistically consistent ($\chi^2=2.1$), with a combined statistical error of ± 0.0015. Within statistical errors the result is also independent of the time of muon decay.

Multiple Coulomb scattering in the production and stopping targets causes a misalignment of the μ^+ spin and momentum, resulting in the measured values of $\cos\theta_\mu$ being systematically too large. An estimated correction of $+0.0012\pm0.0005$ is made to $\xi P_\mu \delta/\rho$. Table 2 summarises the major sources of systematic error. All other sources contribute $<10^{-4}$. In principle the systematic errors should be uncorrelated; in quadrature they add to ± 0.0018. The resulting value is $\xi P_\mu \delta/\rho = 0.9989\pm0.0015\pm0.0018$. We have made no correction for unknown sources of μ^+ depolarisation either along the beam or in the stopping target. Since such effects can only decrease the apparent result, we therefore quote the limit:

$$\xi P_\mu \delta/\rho > 0.9959 \qquad \text{(90\% confidence)}$$

The corresponding limits on the mass and mixing parameters α and ζ are represented by the small bold contour in Fig. 8. In particular, for infinite W_R mass $|\zeta|<0.045$; for any mixing angle $M(W_R)>380$ GeV; and for zero mixing angle $M(W_R)>450$ GeV.

We also note that for a (V+A) amplitude admixture, $(V-A)+\varepsilon(V+A)$, assuming no left-right mixing $\xi P_\mu \delta/\rho \approx 1-4\varepsilon^2$. Our result implies $|\varepsilon|< 0.032$ with 90% confidence.

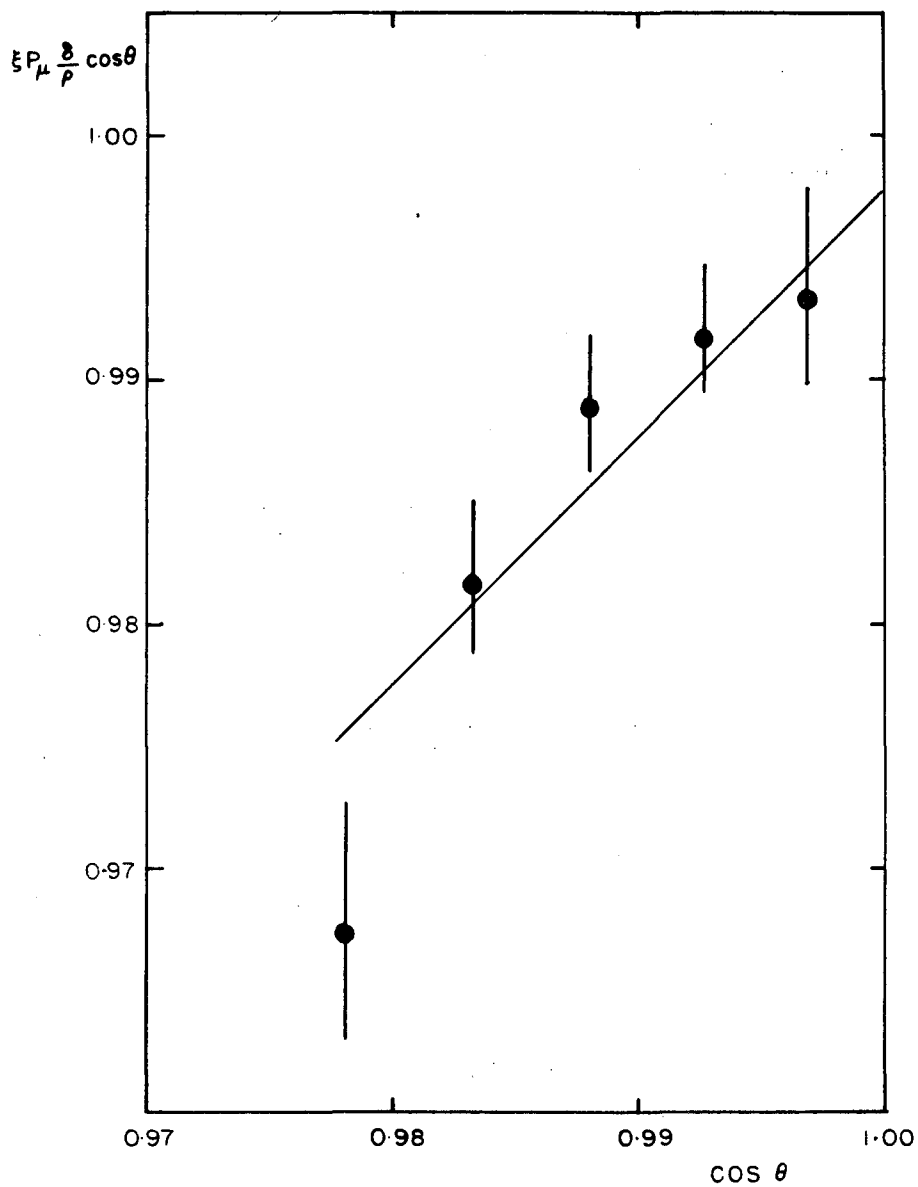

FIG. 6. The fitted values of $(\xi P_\mu \delta/\rho)\langle\cos\theta\rangle$ for data in each of five bins in $\cos\theta$. The errors are statistical. A fixed slope extrapolation to $\cos\theta=1$ is made to determine $\xi P_\mu \delta/\rho$.

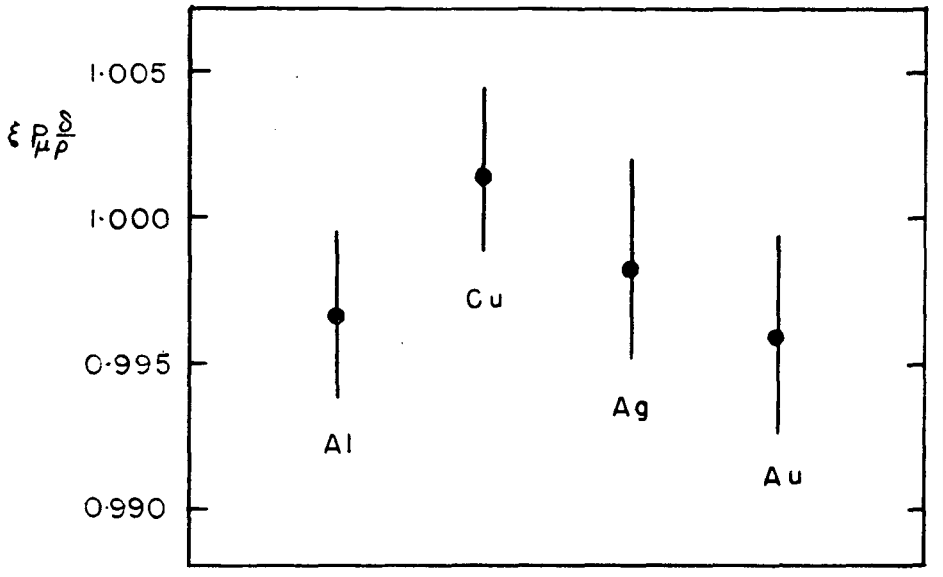

FIG. 7. The fitted values of $\xi P_\mu \delta/\rho$ for each of the four stopping target materials.

TABLE 2.

Major sources of systematic error and their estimated contributions.

Source of systematic error	Error
Coulomb scattering in targets	±0.0005
Correction of θ_μ and θ_e for bending in B_L field at target	±0.0010
Smearing of θ_μ and θ_e due to detector resolution and scattering	±0.0006
Possible shift in θ_e due to random hits and inefficiencies in D1 and D2	±0.0005
Method of averaging $\langle\cos\theta\rangle$	±0.0004
Difference in x=1 edge calibration between B_T and B_L data	±0.0008
Normalisation of B_L relative to B_T data	±0.0007

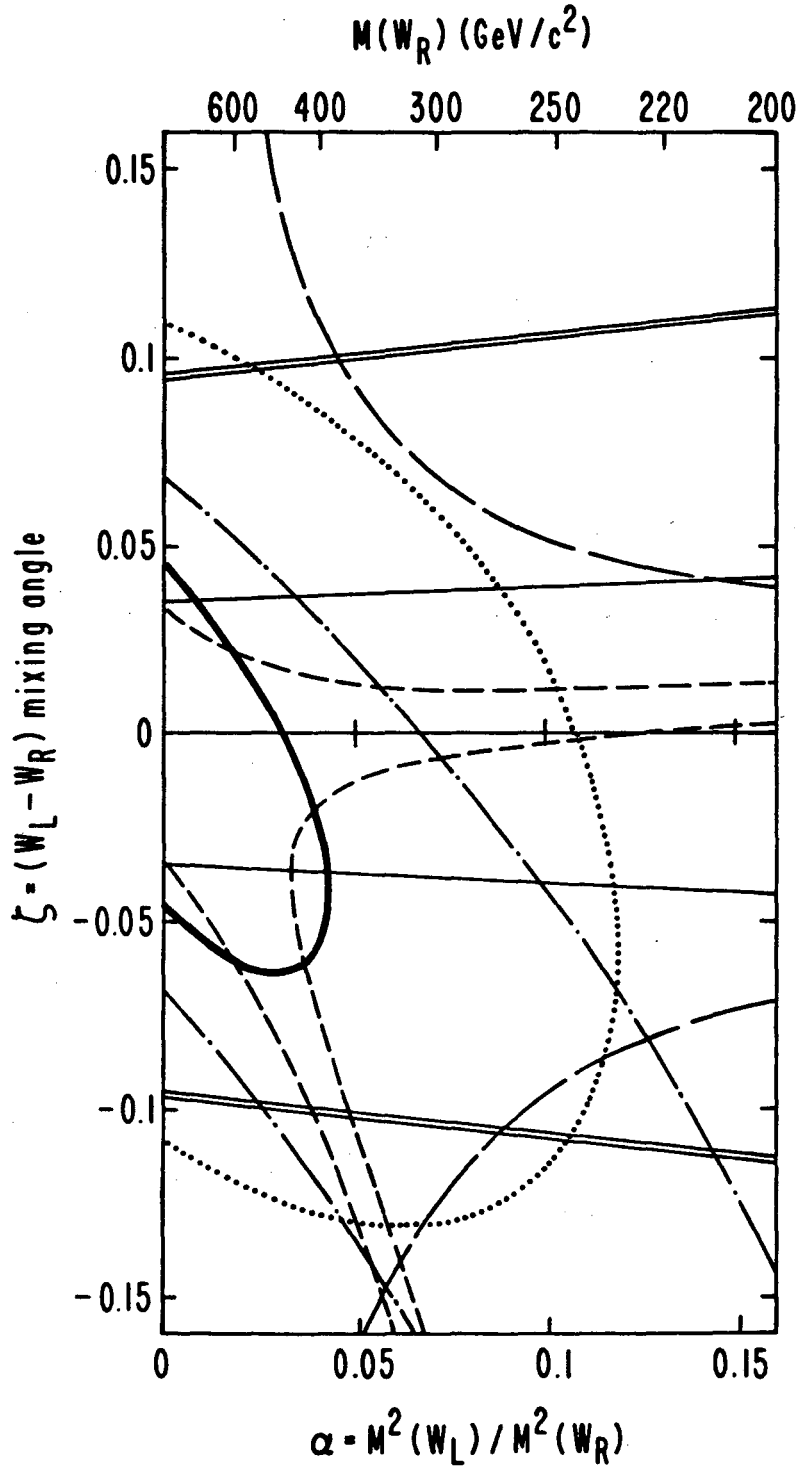

FIG. 8. The small bold contour representing the present result is shown together with the contours of Fig. 1.

B. μSR DATA

The B_T data may be used for an independent measurement of the decay asymmetry. Figures 9 and 10 show the B_L and B_T data time spectra for all target materials combined.

A maximum likelihood fit using Poisson statistics is made simultaneously to 125,000 B_T events and 59,000 B_L events in 115 time bins. For the B_L data, the expected number of events in each time bin is given by:

$$N_L(t) = N_L^o \exp(-t/\tau_\mu) + C_L$$

The B_T data are fitted in four x bins, each 0.02 wide, to the radiatively corrected differential decay rate, assuming (V-A) values for the muon decay parameters η, ρ, and δ. The expected number of events in each time bin is then given by:

$$N_T(t) = N_T^o\left[\int_x A(x)dx + R(t)\langle\cos\theta\rangle_t \xi P_\mu \int_x B(x)dx\right]\exp(-t/\tau_\mu) + C_T$$

where A(x) and B(x) are the angle independent and angle dependent parts of the differential decay rate respectively; $\langle\cos\theta\rangle_t$ is the value of $-\hat{P}_\mu(t).\hat{p}_e$ appropriate to the particular time bin; and

$$R(t) = \exp\{-2\sigma^2\tau_c^2[\exp(-t/\tau_c)-1+t/\tau_c]\}$$

is an effective relaxation function[20] parametrising the effects of slightly different muon spin precession rates due to small variations in the magnetic field strength over the target foil and from run to run.

The $\langle\cos\theta\rangle_t$ are determined from the observed μ^+ and e^+ track

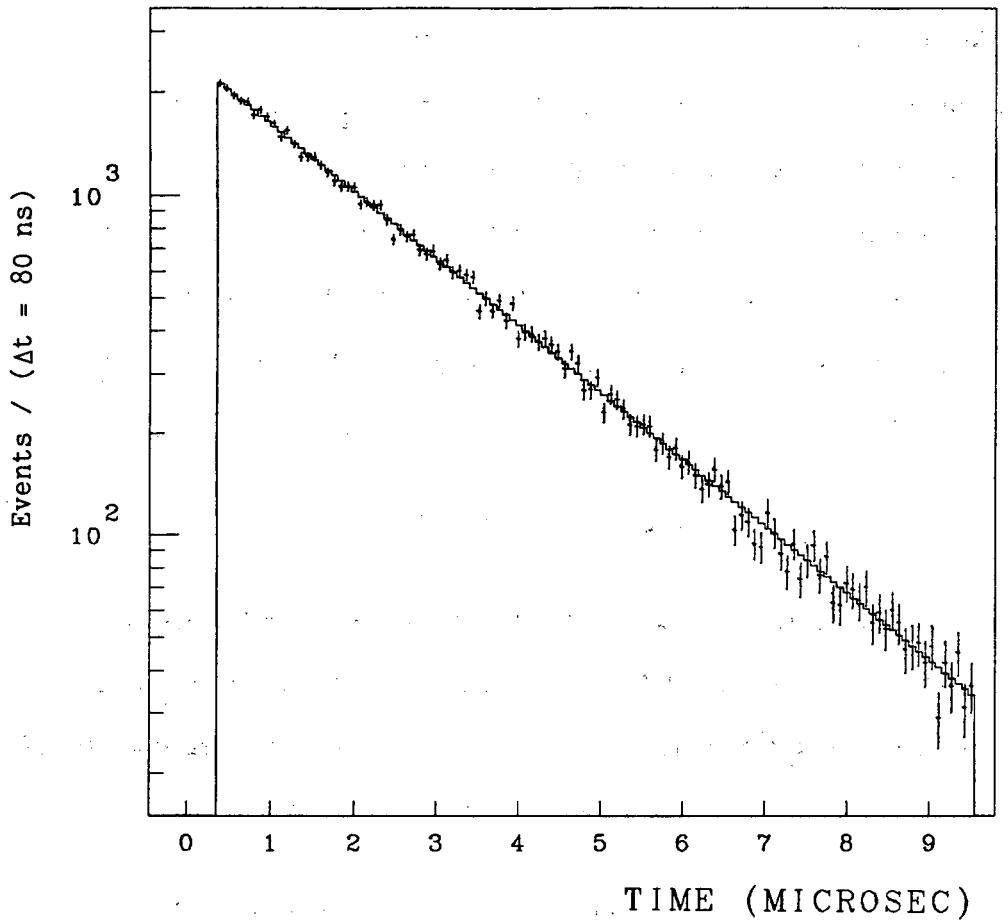

FIG. 9. The time spectrum of the spin-held B_L data with the fit described in the text. The fitted muon life-time, determined simultaneously from the B_L and B_T data, is τ_μ=2.204±0.010±0.044 μs, which is consistent with the accepted value of 2.197 μs. The fitted background is 0.07±1.1.

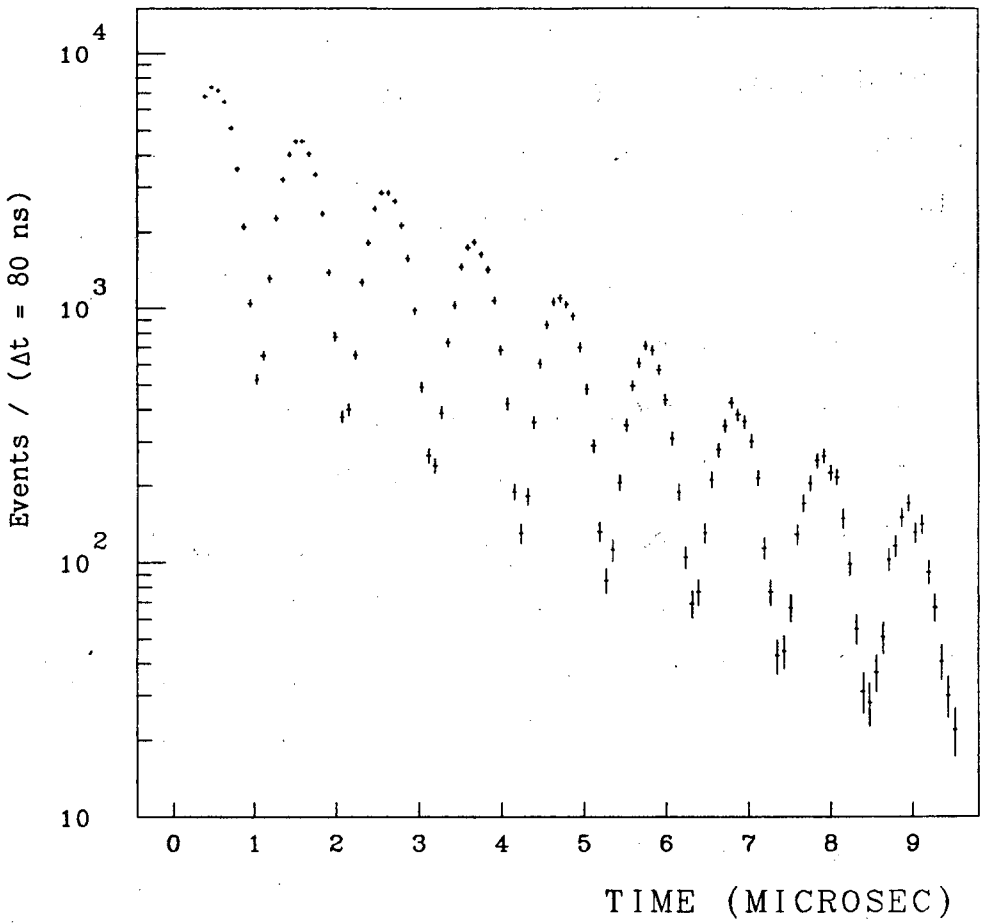

FIG. 10. The time spectrum of the spin-precessed B_T data for all target materials combined. The decay asymmetry is determined from the amplitude of the μSR signal. The small decrease in the signal amplitude with time is due to slightly different muon spin precession rates resulting from small variations in the magnetic field strength over the stopping target and from run to run.

directions at the stopping target in a large part of the B_T data time spectrum for which the decaying muons are, on average, unpolarised. Since the decay of unpolarised muons is isotropic, the observed angular distribution of the e^+ in these events is determined only by the acceptance of the apparatus. Similarly, the observed angular distribution of the incoming μ^+ is determined only by the acceptance of the apparatus and the beam phase-space. Allowing the muon spin precession rate to be a free parameter in the fit then permits an unbiased determination of $\langle\cos\theta\rangle_t=-\hat{P}_\mu(t).\hat{p}_e$ for each time bin by calculating the average $\cos\theta$ for every precessed μ^+ spin direction combined with every outgoing e^+ direction. The resulting fit is shown superimposed on the B_T data in Fig. 11 with the muon life-time dependence removed.

We make corrections for μ^+ multiple Coulomb scattering (+0.0012±0.0005); the effect of an incompletely nulled longitudinal field in the stopping target region (+0.0003±0.0003); and for a small background due to incomplete rejection of additional μ^+ arriving after the μ-stop (-0.0005±0.0005). The resulting value $\xi P_\mu \delta/\rho=0.9970\pm0.0037\pm0.0015$ is consistent with the value obtained from the spin-held data. The smaller systematic error for the μSR data is mainly due to less uncertainty in determining the μ^+ and e^+ momenta directions in the absence of the 1.1 T longitudinal field.

The 90% confidence limit $\xi P_\mu \delta/\rho>0.9918$ for these data implies that for infinite W_R mass $|\zeta|<0.064$; for any mixing angle $M(W_R)>320$ GeV; and for zero mixing angle $M(W_R)>380$ GeV.

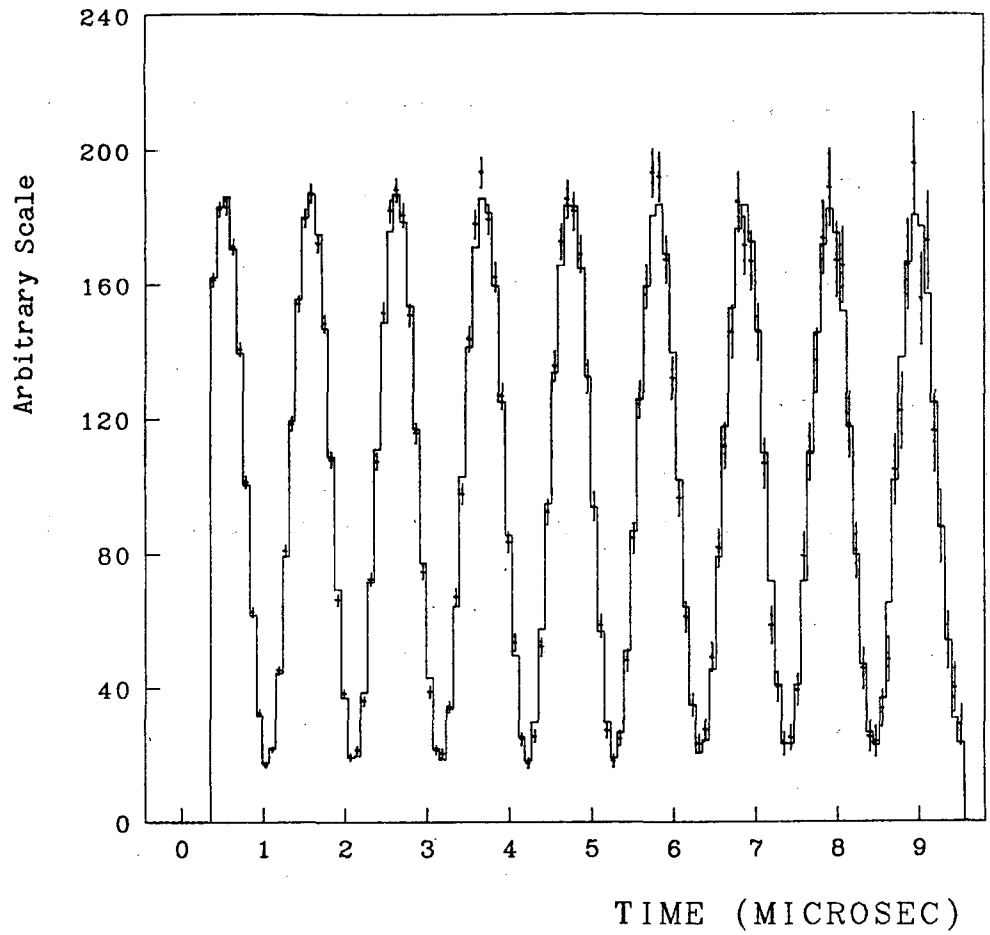

FIG. 11. The time spectrum of the spin-precessed data, after removal of the muon life-time dependence, shown together with the maximum likelihood fit. The ordinate scale is arbitrary.

LIMITS ON SCALAR AND TENSOR CURRENTS

The most general four-fermi interaction for muon decay may be written in flavor retention form as

$$L_{int} = -(G_F/\sqrt{2})\sum_i(\bar{e}\Gamma_i\nu_e)[\bar{\nu}_\mu\Gamma_i(G_i+G_i'\gamma_5)\mu] + \text{hermitian conjugate}$$

where $\Gamma_i = 1, \gamma_\lambda, \sigma_{\lambda\kappa}, \gamma_\lambda\gamma_5, i\gamma_5$.

Time reversal invariance requires the G_i and G_i' to be real. Fierz transforming to the charge retention form then leads to the following relations between $\xi\delta/\rho$ and the G_i and G_i' for the special cases of flavor retention scalar or tensor admixtures to (V-A):

1. (V-A) + tensor: $\xi\delta/\rho \approx 1-(G_T+G_T')^2/8$
2. (V-A) + scalar + pseudoscalar: $\xi\delta/\rho \approx 1-[(G_S-G_P')^2+(G_S'-G_P)^2]/16$

Hence from our result $\xi\delta/\rho \geq \xi P_\mu\delta/\rho > 0.9959$ we obtain the 90% confidence limits:

$$(G_T+G_T')^2 < 0.033$$

$$(G_S-G_P')^2+(G_S'-G_P)^2 < 0.066$$

Mursula et al.[21] have set limits based on all previous available data subject to various sets of assumptions, all somewhat different from those used to determine our limits.

LIMITS ON FAMILONS

Recently, Wilczek[22] has suggested replacing the Peccei-Quinn U(1) quasisymmetry with a group of genuine flavor symmetries. Spontaneous breakdown of family symmetries would involve characteristic massless axion-like Nambu-Goldstone bosons $f_{\ell\ell'}$ (familons) coupling to the divergences of currents which change flavor quantum numbers.

The decay $\mu \to e+f$ could then occur via

$$\Delta L = (1/F_{\mu e})\bar{\mu}\gamma_\rho e \partial_\rho f_{\mu e}$$

with a branching ratio $\Gamma(\mu\to ef)/\Gamma(\mu\to e\nu\bar{\nu}) = 2.5\times10^{14}\mathrm{GeV}^2/F^2_{\mu e}$ where $F_{\mu e}$ is the energy scale at which the flavor symmetry is spontaneously broken. It was further suggested on cosmological grounds that 10^9 GeV $< F_{\mu e} < 10^{14}$ GeV implying

$$2.5\times10^{-10} < \Gamma(\mu\to ef)/\Gamma(\mu\to e\nu\bar{\nu}) < 2.5\times10^{-4}$$

Since $\mu\to ef$ is isotropic and M(f)=0, the clearest evidence for this decay in our experiment would be the observation of a spike at the end point of the momentum spectrum for polarised μ^+ decay opposite to the muon spin direction, where the V-A rate vanishes.

Fitting the spin-held data with various assumed $\mu\to ef$ branching ratios yields the limit

$$\Gamma(\mu\to ef)/\Gamma(\mu\to e\nu\bar{\nu}) < 6\times10^{-6}$$

and

$$F_{\mu e} > 4.2\times10^{10}\ \mathrm{GeV}$$

LIMITS ON COMPOSITE LEPTONS

The possibility that leptons and quarks are composite at some mass scale Λ has recieved considerable attention in recent years. Among the strongest experimental limits on Λ currently quoted[23,24] are those from Bhabba scattering (>750 GeV), muon (g-2) (>860 GeV), and a more model-dependent estimate from ν-hadron scattering (>2.5 TeV).

The effects of compositeness may be analysed in terms of new effective contact interactions. Following the analyses of Peskin,[25] and Lane and Barany[26] the most general SU(2)×U(1) invariant contact interaction contributing to $\mu \to e\nu\bar{\nu}$ is

$$\begin{aligned} L_{cont} = (g^2/\Lambda^2)[&\eta_1(\bar{\nu}_{\mu L}\gamma^\kappa\mu_L)(\bar{e}_L\gamma_\kappa\nu_{eL}) + \eta_2(\bar{\nu}_{\mu R}\gamma^\kappa\mu_R)(\bar{e}_R\gamma_\kappa\nu_{eR}) \\ &+ \eta_3(\bar{\nu}_{\mu L}\gamma^\kappa\nu_{eL})(\bar{e}_R\gamma_\kappa\mu_R) + \eta_4(\bar{e}_L\gamma^\kappa\mu_L)(\bar{\nu}_{\mu R}\gamma_\kappa\nu_{eR}) \\ &+ \eta_5(\bar{\nu}_{\mu L}\mu_R)(\bar{e}_L\nu_{eR}) + \eta_6(\bar{\nu}_{\mu L}\nu_{eR})(\bar{e}_L\mu_R) \\ &+ \eta_7(\bar{\nu}_{\mu R}\mu_L)(\bar{e}_R\nu_{eL}) + \eta_8(\bar{\nu}_{\mu R}\nu_{eL})(\bar{e}_R\mu_L)] \end{aligned} \tag{3}$$

where g is a coupling of hadronic strength; the η_i are of order unity and are normalised so that $|\eta_L|=1$ in the diagonal coupling

$$(g^2/2\Lambda^2)[\eta_L(\bar{e}_L\gamma^\kappa e_L)(\bar{e}_L\gamma_\kappa e_L) + \ldots]$$

The first and second terms in (3) are purely left-handed and right-handed respectively, and hence are indistinguishable from the usual (V-A) and (V+A) interactions.

There are three special cases of interest:

1. If only left-handed (right-handed) leptons are composite then only the purely left-handed (right-handed) term survives, i.e. only η_1 (η_2) $\neq 0$.

2. If both left-handed and right-handed leptons are composite but contain quite different sets of constituents then the purely left-handed and right-handed terms dominate, i.e. $\eta_1, \eta_2 >>$ other η_i.

3. If there is no ν_R, or $M(\nu_R)$ is very large, only $\eta_1, \eta_3 \neq 0$.

Assuming an effective interaction Lagrangian

$$L_{eff} = L_{V-A} + L_{cont}$$

we obtain [cf (2)] the end point decay rate

$$R(1,0) = 2(620\text{GeV}/\Lambda)^4 (g^2/4\pi)^2 (\eta_2^2+\eta_3^2+\eta_5^2/4)$$

Our limit $R(1,0)=1-\xi P_\mu \delta/\rho<0.0041$ then implies

$$\Lambda^2 > (2920\text{GeV})^2 (g^2/4\pi)\sqrt{(\eta_2^2+\eta_3^2+\eta_5^2/4)}$$

with 90% confidence. (If the not unreasonable assumptions $g^2/4\pi \approx 2.1$ and $\eta_i > 0.2$ are made, the limit $\Lambda > 2300$ GeV would be obtained.)

For the special cases discussed earlier the limit becomes

1. Only left-handed leptons composite: no limit
2. Left and right-handed leptons have different sets of constituents: $\Lambda^2 > (2920\text{GeV})^2 (g^2/4\pi)\eta_2$
3. No ν_R, or $M(\nu_R)$ very large: $\Lambda^2 > (2920\text{GeV})^2 (g^2/4\pi)\eta_3$

PROSPECTS

The results presented here are based on the data collected during the first run of the experiment. Analysis of about three times as much data from the second run should be completed in late 1983.

A third and final run of the experiment is scheduled for early 1984. The run will be partially devoted to measuring the muon decay parameter δ to a proposed $\sigma(\delta)=0.003$. The μSR mode will be used to measure the decay asymmetry over the reduced momentum range $x=0.4$ - 1.0.

Any theory with two-component neutrinos has $\delta=3/4$. This is also the case in the left-right symmetric model $SU(2)_L \times SU(2)_R \times U(1)$. However, theories with heavy neutrinos such as the fermion-mirror fermion mixing models,[27] which arise from the 'big' gauge groups SO(n) with n>10 or SU(n) with n>5, predict values of δ different from 3/4. Hence a measurement of δ can be used, together with measurements of other quantities, to constrain the parameters of these theories.

In addition, measurement of the decay asymmetry over a much wider range of x than previously will allow sensitivity to right-handed currents if $M(\nu_R)<50$ MeV.

This research was supported in part by the U.S. Department of Energy through Contracts No. DE-AC03-76SF00098 and AC02-ER02289.

REFERENCES

1. J.C. Pati and A. Salam, Phys. Rev. Lett. 31, 661 (1973) and Phys. Rev. D10, 275 (1974);
   R.N. Mohapatra and J.C. Pati, Phys. Rev. D11, 566 and 2588 (1975)
2. M.A.B. Beg et al., Phys. Rev. Lett. 38, 1252 (1977).
3. B.R. Holstein and S.B. Treiman, Phys. Rev. D16, 2369 (1977).
4. The primary input to the world average is V.V. Akhmanov et al., Yad. Fiz. 6, 316 (1967).
5. The primary input to the world average is J. Peoples, Nevis Cyclotron Report No. 147 (1966).
6. J. Van Klinken, Nucl. Phys. 75, 145 (1966).
7. J. Van Klinken et al., Phys. Rev. Lett. 50, 94 (1983).
8. D. Schreiber and F.T. Calaprice, private communication;
   D. Schreiber, Ph.D. Thesis, Princeton University, 1983 (unpublished). We calculated the contour plotted in Fig. 1 using A(0)=0.0363±0.0008; ft ratio=1.797±0.002. See also F.T. Calaprice et al., Phys. Rev. Lett. 35, 1566 (1975).
9. H. Abramowicz et al., Z. Phys. C12, 225 (1982)
10. M. Gell-Mann, P. Ramond and R. Slansky, unpublished.
11. R.N. Mohapatra and G. Senjanovic, Phys. Rev. Lett. 44, 912 (1980) and Phys. Rev. D23, 165 (1981).
12. J. Carr et al., Phys. Rev. Lett. 51, 627 (1983).
13. G. Beall, M. Bander and A. Soni, Phys. Rev. Lett. 48, 848 (1982).
14. P. DeForcrand, Ph.D. Thesis, Univ. of. Calif., Berkeley (1982), LBL-14692.
15. R.N. Mohapatra et al., Phys. Rev. D28, 546 (1983).

16. M. Denis, Phys. Rev. D28, 1219 (1983).

17. F. Scheck, Phys. Lett. C44, 187 (1978); A.M. Sachs and A. Sirlin, in Muon Physics, Vol. II, V. Hughes and C.S. Wu, eds. (Academic Press, N.Y., 1975), p. 50.

18. A.E. Pifer et al., Nucl. Inst. Meth. 135, 39 (1976).

19. C.J. Oram et al., Nucl. Inst. Meth. 179, 95 (1981).

20. A. Abragam, The Principles of Nuclear Magnetism [Oxford Uni. Press (Clarendon), London and N.Y., 1970]

21. K. Mursula et al., Nucl. Phys. B219, 321 (1983).

22. F. Wilczek, Phys. Rev. Lett. 49, 1549 (1982).

23. M. Abolins et al., Proc. 1982 DPF Summer Study Elem. Part. Phys. and Future Facilities p.274 (Snowmass, 1982).

24. E.J. Eichten et al., Phys. Rev. Lett. 50, 811 (1983).

25. M.E. Peskin, private communication.

26. K.D. Lane and E. Barany, private communication.

27. J. Maalampi et al., Nucl. Phys. B207, 233 (1982).

This report was done with support from the Department of Energy. Any conclusions or opinions expressed in this report represent solely those of the author(s) and not necessarily those of The Regents of the University of California, the Lawrence Berkeley Laboratory or the Department of Energy.

Reference to a company or product name does not imply approval or recommendation of the product by the University of California or the U.S. Department of Energy to the exclusion of others that may be suitable.

TECHNICAL INFORMATION DEPARTMENT
LAWRENCE BERKELEY LABORATORY
UNIVERSITY OF CALIFORNIA
BERKELEY, CALIFORNIA 94720